Materials Science Forum Vols. 539-543 (2007) pp. 1983-1987
online at http://www.scientific.net
© (2007) Trans Tech Publications, Switzerland

X-ray Study Of $Pd_{40}Cu_{30}Ni_{10}P_{20}$ Bulk Metallic Glass Brazing Filler For Ti-6Al-7Nb Alloy

E. Miura[1, a], G.E. Ice[2, b], E. D. Specht[2, c], J.W.L. Pang[2, d], H. Kato[3, e], K. Hisatsune[1, f], I. Inoue[3, g]

[1] Division of Dental and Biomedical Materials Science, Graduate School of Biomedical Sciences Nagasaki University, 1-7-1 Sakamoto, Nagasaki 852-8588, Japan

[2] Oak Ridge National Laboratory, Oak Ridge, TN 37831-6118, USA

[3] Institute for Materials Research, Tohoku University, 2-1-1 Katahira, Aoba-ku, Sendai 980-8577, Japan

[a] fujiwarae@ornl.gov, [b] icege@ornl.gov, [c] spechted@ornl.gov, [d] pangj@ornl.gov, [e] hikato@imr.edu, [f] hisatune@net.nagasaki-u.ac.jp, [g] ainoue@imr.tohoku.ac.jp

keywords: brazing, metallic glass, titanium alloy, crystalline, x-ray microdiffraction, x-ray microfluorescence

Abstract. Crystalline precipitates in a bulk-metallic-glass (BMG) braze were investigated with an intense x-ray microbeam. The precipitates were found in the $Pd_{40}Cu_{30}P_{20}Ni_{10}$ BMG braze matrix after joining crystalline Ti-6Al-7Nb. However, the role (if any) played by the precipitates in improving the mechanical bond of the BMG/crystalline joint is unknown. X-ray microdiffraction and microfluorescence measurements from small sample volumes were made with an ~ 0.5 x 0.5 μm^2 beam. Spatially-resolved Laue diffraction and x-ray fluorescence measurements were made on several second-phase crystals within the BMG matrix. Although precipitate crystals with the observed compositions were anticipated to be predominantly hexagonal, one of the crystals was found to be cubic or tetragonal. The instrumentation includes capabilities for 3D depth-resolved measurements of crystal structure and for fluorescence analysis of elemental composition. Depth profiling gave information about the grain distribution and morphology in the BMG matrix.

Introduction

Ti and Ti alloys are emerging as important materials for dental and medical applications; they are inherently biocompatible with excellent physical, mechanical and chemical properties. Ti-based metals are commonly used for load-bearing dental applications including crowns, dentures, orthodontic devices and endosseous implants. The Ti-6Al-7Nb alloy was specifically developed as a biomedical alternative to Ti-6Al-4V [1-3] but deployment of this alloy to many biomedical applications is dependent on the development of biocompatible joining techniques.

Joining is a major challenge of processing dental devices using Ti alloys. Joining is required for relatively large Ti dental devices because of the poor conformity of Ti alloys and / or when dental bridges are made with different alloy types. For dental applications, infrared (IR) joining is often used for brazing Ti and its alloys; infrared joining is well established, is low cost, and limits oxidation during joining of high-melting-point Ti alloys. Brazing of Ti and its alloys requires brazing filler metal, with high corrosion resistance, adequate joint strength, short processing time to avoid oxidation, a melting point that is lower than the transformation temperature, good biocompatibility, and no toxicity.

Bulk metallic glasses (BMG) have been proposed as a candidate brazing filler for Ti alloys, since their melting temperatures are lower than that of conventional Ti-Cu-Ni plating strips [4], and BMGs have an intrinsically uniform microstructure. In addition, many kinds of BMG have excellent mechanical properties including good corrosion resistance. Some researchers have attempted to apply Zr-Ti-Cu based amorphous alloys as a brazing filler [5, 6], and they indicated metallic glass has excellent filler properties.

Our previous results showed that $Pd_{40}Cu_{30}Ni_{10}P_{20}$ BMG / Ti-6Al-7Nb joints have high strength and excellent corrosion resistance. After mechanical loading, fracture was found to occur at a reaction layer of the $Pd_{40}Cu_{30}Ni_{10}P_{20}$ / Ti-6Al-7Nb interface. In addition, the corrosion resistance of the joint appears to be similar to that of the Ti-6Al-7Nb and superior to the original $Pd_{40}Cu_{30}Ni_{10}P_{20}$ filler material. SEM analysis observed, that after brazing, the metallic glass filler

All rights reserved. No part of contents of this paper may be reproduced or transmitted in any form or by any means without the written permission of the publisher: Trans Tech Publications Ltd, Switzerland, www.ttp.net. (ID: 160.91.159.140-20/11/06,20:39:57)

includes submicroscopic maple-leaf-shaped primary grains and peritectic grains in a glassy matrix with a complex reaction layer at the interface. However, the relationship between the mechanical and chemical properties and the embedded microstructure it is not well understood. Due to the small brazing area and small volume fraction of the primary and peritectic grains in the filler metal, it is difficult to identify its crystal structure by conventional or micro-area X-ray diffractometry.

Thus, in this study, microstructures of a Ti-6Al-7Nb alloy brazed with $Pd_{40}Cu_{30}Ni_{10}P_{20}$ metallic glass filler were investigated with a new method: polychromatic microdiffraction. Second-phase crystal structures in the glassy phase matrix were probed with an intense synchrotron microbeam. X-ray microdiffraction measurements from small sample volumes were made with an ~ 0.5 x 0.5 μm^2 beam. The instrumentation includes capabilities for 3D depth-resolved measurements of crystal structure [7] and for fluorescence analysis of elemental composition. Submicron spatially-resolved Laue diffraction and x-ray fluorescence measurements were made on several second-phase crystals within the BMG matrix [8]. Depth profiling gave information about the grain distribution and morphology in the BMG matrix.

Experimental Procedures

Materials and Brazing Procedure. $Pd_{40}Cu_{30}Ni_{10}P_{20}$ was cast in a cylindrical shape with 2 - 3 mm diameter by arc melting. Cast metal was cut into an appropriate size for brazing, and was cleaned with acetone. A Ti-6Al-7Nb ingot (Ti:Al:Nb = 86.5:6.0:7.0 mass%) was used for brazed metal. The ingot has a forged microstructure consisted with equiaxed α (hcp) and lamellar α (hcp) + ® (bcc) phase. The ingot was sliced into 3.0*w* x 0.8*t* x 30*l* mm^3 plates using a diamond cutting wheel. The plates were used for a butt joint. The fusion face of the plates was mechanically polished by #1500 emery paper and cleaned with acetone.

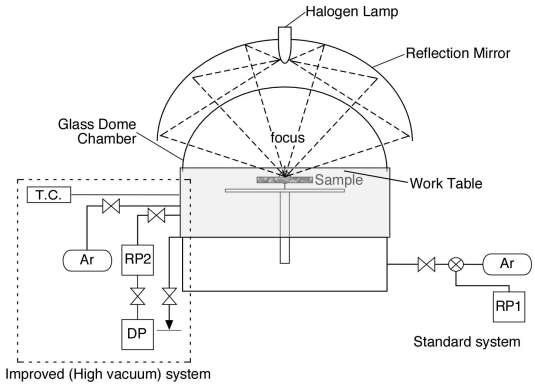

Fig. 1 Schematic illustration of IR brazing machine.

A pair of Ti-6Al-7Nb plates for a butt joint were fixed at their edges on a Co-Cr jig, and BMG filler was pre-placed in the gap. A low temperature brazing flux for precious alloys was applied for brazing. Preplaced brazing of the butt joint was performed using an infrared (IR) brazing machine in an Ar atmosphere as Fig. 1 illustrates. After pre-evacuation in the vacuum of less than 2 x 10^{-3} Pa, brazing was carried out in the Ar atmosphere of 0.5 x 10^5 Pa, and then Ar gas was induced at a side of the specimen. The cooling rate at 700 K is about 25 K/s for a brazing temperature of 800 K.

Microstructure observation. After brazing, cross-sectional microstructural studies of brazed filler were carried out. The brazed butt joint was cut perpendicular to the fusion face by a diamond-cutting wheel, and then its cross-section was polished by colloidal silica.

The cross-section of the joint was observed using an optical microscope (OM), a scanning electron microscope with energy dispersive X-ray spectroscopy (SEM-EDS) and an electron probe microanalyzer (EPMA).

Synchrotron X-ray studies. Fig. 2 a) shows a schematic illustration of powder diffraction measurement and characteristic X-ray mapping. The specimen surface was placed at an angle of about 5 degrees from the incident beam with an energy-dispersive detector upstream of the sample, and an X-ray CCD camera for powder diffraction set nominal to incident beam and behind the specimen. A monochromatic beam was used for these measurements. X-ray Laue diffraction was

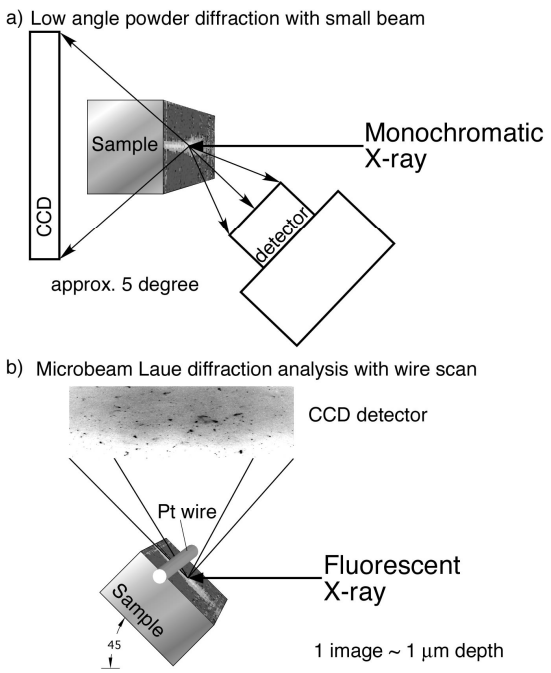

Fig. 2 Schematic illustrations of a) powder diffraction and chemical analysis by small monochromatic beam and b) microbeam analysis with wire scan.

taken at selected positions.

Microbeam Laue diffraction measurements were carried out as illustrated in Fig 2 b). The specimen was set at an angle of 45 degree to the incident white beam, with a CCD camera placed above the specimen. The angle between the incident beam and the CCD camera is 90 degree. When depth profile of the grain is taken, wire scan is carried out simultaneously. The position of the target grain was determined using characteristic X-rays and an optical long-distance microscope. Monochromatic energy scans of the incident beam were carried out to determine the energy of each Laue spot.

Results and discussion

Microstructure of the brazing filler. Fig. 3 shows an optical microscopic (OM) image of $Pd_{40}Cu_{30}Ni_{10}P_{20}$ / Ti-6Al-7Nb brazing zone and a backscattering electron (BSE) image of its interface between base metal and brazing filler metal. Reaction layers are observed at the interface between the base metal and the brazing filler. Primary grains, which are fragmented "maple-leaf" dendrite, and peritectic (or peritectoid) precipitate close to the interface within the matrix. The dendrites are surrounded by peritectic, and the average grain size of the primary grains is about 5 μm. The filler matrix appears to be uniform, in addition, powder diffraction image in Fig. 4 indicates the matrix is primarily a glassy phase. Table 1 shows the chemical composition of the base metal, the filler matrix, the primary grains and the peritectic grains. The matrix and the grains contain Pd, Cu, Ni, and P, and these chemical compositions are almost the same as the original $Pd_{40}Cu_{30}Ni_{10}P_{20}$ BMG. On the other hand, a certain fraction of Ti is also detected in the primary grains. Compared with the matrix, Ni, Ti and P content increases and Cu and Pd decrease in the primary grains, and Pd and Cu increase in the peritectic. In addition, pore containing grains are observed.

a). OM image of brazing zone

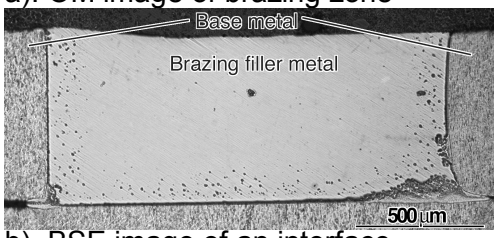

b). BSE image of an interface

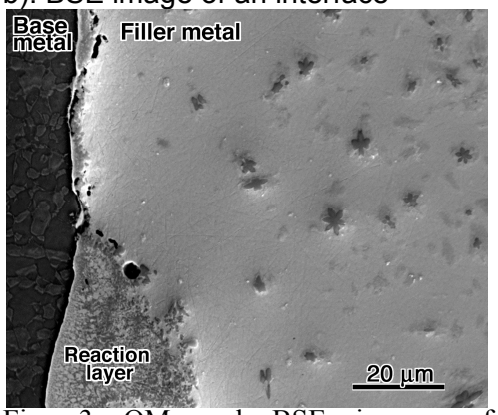

Fig. 3 OM and BSE images of $Pd_{40}Cu_{30}Ni_{10}P_{20}$ / Ti-6Al-7Nb brazing zone.

Table 1 Chemical composition of base metal, $Pd_{40}Cu_{30}Ni_{10}P_{20}$ matrix, and precipitations in the brazing filler.

mol%	Base metal	Filler		
		Matrix	peritectic grain	primary grain
Pd	-	42.76	31.92	10.95
Ni	0.026	8.573	11.26	34.18
Cu	0.001	29.46	42.68	2.900
P	-	19.08	14.01	31.85
Al	16.29	0.074	0.070	0.046
Ti	80.36	0.017	0.049	19.57
Nb	3.322	0.035	0.003	0.504
total	99.999	99.999	99.992	100

Therefore, from the chemical composition of the grain in the filler, it is indicated that elements in the base metal, especially Ti, dissolved into the filler metal at the interface during brazing. Considering the shape and distribution of dendrites, the fragment dendrites are considered to be formed due to precipitation and separation of the crystals from the interface. That is, at an initial stage of solidification, crystals containing Ti might be formed at interface and separate from the interface owing to compositional depression of undercooling at the interface, and then crystal growth and multiplication might occur due to temperature fluctuation and / or segregation in the vicinity of the interface.

Since critical cooling rate of $Pd_{40}Cu_{30}Ni_{10}P_{20}$ BMG is about 0.1 K/s [9], the applied cooling rate is high enough for metallic glass formation although additional element such like Ti tend to lower the glass formation ability.

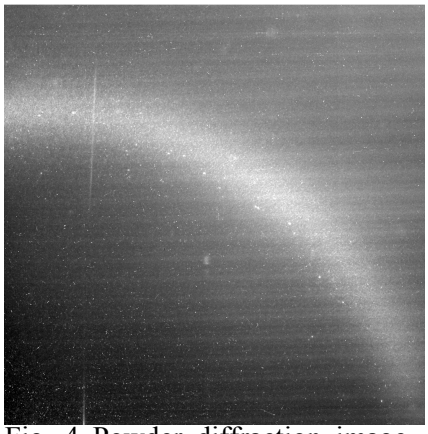

Fig. 4 Powder diffraction image of a filler matrix.

Grain characterization by monochromatic beam. Elemental maps near a grain are shown in Fig. 5. Based on the chemical distribution the position of the precipitates with anomalous chemistry is precisely detected. The map contrast is set for white to indicate higher concentration than dark area. Ti-rich but Pd-poor area, Ti-rich area and Cu-rich areas are observed in this area. Compared with EPMA results, Ti-rich Pd-poor area is considered as an indicator of a primary grain. From micro area XRD measurements, the existence of an hcp structure was indicated, however, indexation of Laue diffraction patterns suggests that there might also be an fcc or fct crystal in this map.

In order to determine the unknown crystal structure, monochromatic energy scans of Laue spot were carried out. Fig. 6 shows the Laue image of a measured primary grain.

The reciprocal vector for each Laue spot can be obtained from its d-spacing and reflection direction. Fig. 7 shows 2D hkl plot of the micro Laue spots analyzed by the energy scan. Almost all spots are on integer values of hkl. According to the measured reciprocal lattice, a primitive lattice can be determined as monoclinic, which is close to hexagonal with small

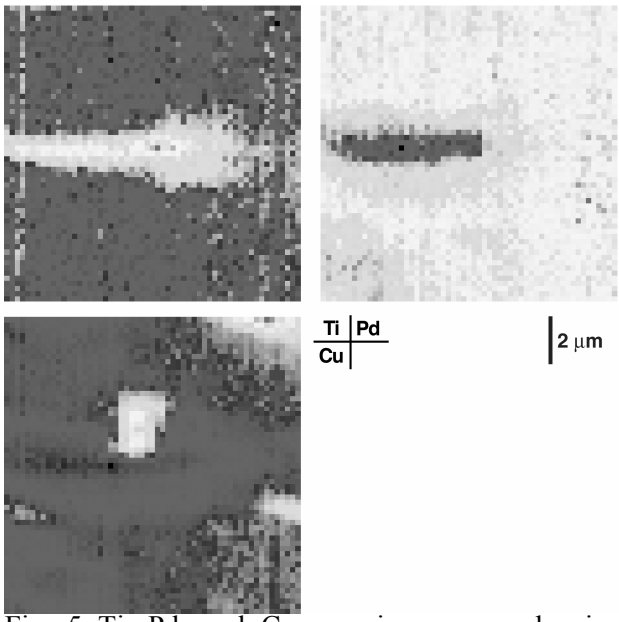

Fig. 5 Ti, Pd, and Cu mapping measured using monochoromatic beam. Whiter dot indicates higher concentration of the element.

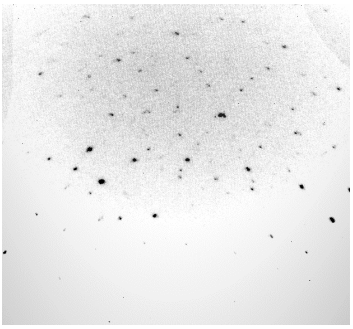

Fig. 6 Laue image of the measured grain in the brazing filler.

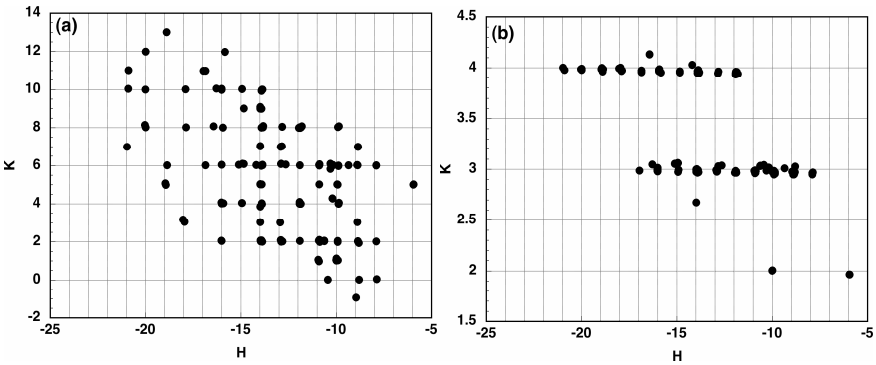

Fig. 7 HKL plots (a: H-K, b: H-L) of the micro Laue spots analyzed by

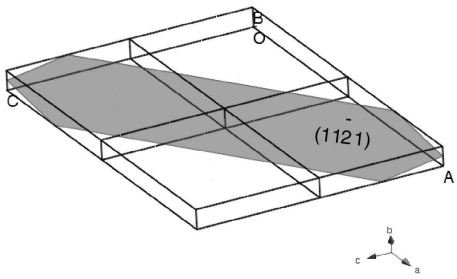

Fig. 8 Four hexagonal unit cells obtained in this study.

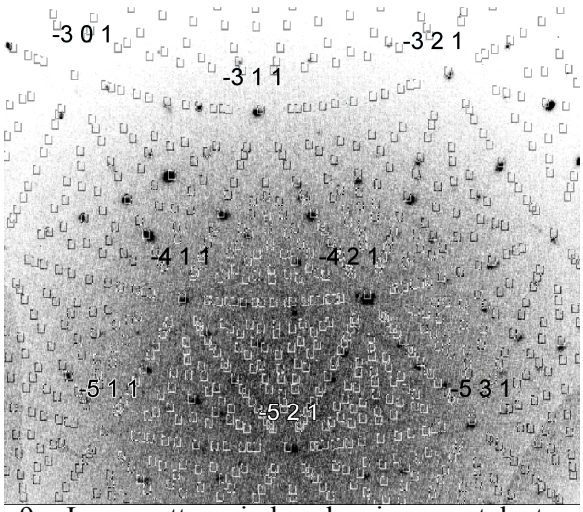

Fig. 9 Laue pattern indexed using crystal structure obtained in this study.

c/a (= 0.23 - 0.25) as shown in Fig. 8. Lattice parameter obtained in this study are, a = 14.0 Å, c = 13.8 Å, b = 3.52 Å, α = 90, β = 120, γ = 90. Fig. 9 is an indexed Laue pattern using the crystal structure obtained in this study. This result shows good agreement between the calculated and measured value.

Summary

This study focused on understanding the origin, structure and consequence of crystalline precipitates in a BMG braze. Evidence from the location and chemistry of the primary grains indicates that Ti diffusion lowers the crystallization temperature and induces local precipitation with subsequent segregation of the Ti to the crystalline regions. X-ray diffraction measurements indicate that several crystal phases are present in the material with different unit cells. Measurements are now underway to refine the crystal structure.

Acknowledgements

Work sponsored by the U.S. Department of Energy (DOE), Division of Materials Sciences and Engineering. Oak Ridge National Laboratory (ORNL) is operated by UT-Battelle, LLC, for the U.S. Department of Energy under contract DE-AC05-00OR22725. Experiments were performed on UNICAT beamline 34-ID at the Advanced Photon Source, Argonne IL. Both 34-ID and the APS are supported by the DOE Office of Basic Energy Science.

The submitted manuscript has been authored by a contractor of the U.S. Government under contract No. DE-AC05-00OR22725. Accordingly, the U.S. Government retains a nonexclusive, royalty-free license to publish or reproduce the published or reproduce the published form of this contribution, or allow others to do so, for U.S. Government purposes.

This work was also partly supported by Grant-in-Aid for Scientific Research from the Ministry of Education, Culture, Sports, Science and Technology (MEXT) Japan under contract No.14771097 and No. 16039216. The authors thank Daido Steel Co. Ltd. for providing material.

References

[1] G. Welsch and E. W. Collings: *Materials Properties Handbook*. (ASM International 1995).

[2] Daido Steel: *APPLICATION OF DAT67 Titanium Alloy IN DENTISTRY* in Daido's Titanuim and Titanium Alloy, http://www.daido.co.jp/products/titanium/dat67.html.

[3] M. Niinomi: Metall. Mater. Trans., vol. 33, (2002), p. 477.

[4] E. Miura, I. Watanabe, K. Hisatsune, and S. Hanada: *Proceedings of Fourth Pacific Rim Int. Conf. on Advanced Materials and Processing (PRICM4)*. (Japan Inst. Metals, 2001), p. 261.

[5] O. Botstein and A. Rabinkin: Metar. Sci. Eng. A, vol. A188, (1994), p. 305.

[6] T. Onzawa, A. Suzumura, and M. W. Ko: Weld. J., vol. 69, (1990), p. 462s.

[7] B. C. Larson, W. Yang, G. E. Ice, J. D. Budai, and J. Z. Tischler: Nature, vol. 415, (2002), p. 887.

[8] J. S. Chung and G. E. Ice: Journal of Applied Physics, vol. 86, (1999), p. 5249.

[9] A. Inoue: Acta Materialia, vol. 48, (2000), p. 279.